

*This is the peer reviewed version of the following article:*

L. Caizán-Juanarena, M. Arnaiz, E. Gucciardi, L. Oca, E. Bekaert, I. Gandiaga, J. Ajuria, Unraveling the Technology behind the Frontrunner LIC ULTIMO to Serve as a Guideline for Optimum Lithium-Ion Capacitor Design, Assembly, and Characterization. *Adv. Energy Mater.* 2021, 11, 2100912.

*, which has been published in final form at*

<https://doi.org/10.1002/aenm.202100912>

*This article may be used for non-commercial purposes in accordance with Wiley Terms and Conditions for Use of Self-Archived Versions.*

*This article may not be enhanced, enriched or otherwise transformed into a derivative work, without express permission from Wiley or by statutory rights under applicable legislation.*

*Copyright notices must not be removed, obscured or modified.*

*The article must be linked to Wiley's version of record on Wiley Online Library and any embedding, framing or otherwise making available the article or pages thereof by third parties from platforms, services and websites other than Wiley Online Library must be prohibited.*

## Unraveling the Technology behind the Frontrunner LIC ULTIMO® to Serve as a Guideline for Optimum Lithium-ion Capacitor Design, Assembly and Characterization

Leire Caizán-Juanarena<sup>1</sup>, María Arnaiz<sup>1</sup>, Emanuele Gucciardi<sup>1</sup>, Laura Oca<sup>1</sup>, Emilie Bekaert<sup>1</sup>, Iñigo Gandiaga<sup>2</sup>, Jon Ajuria<sup>1, \*</sup>

Dr. Leire Caizán, Dr. María Arnaiz, Dr. Emanuele Gucciardi, Dr. Emilie Bekaert, Dr. Jon Ajuria

Centre for Cooperative Research on Alternative Energies (CIC energiGUNE), Basque Research and Technology Alliance (BRTA), Alava Technology Park, Albert Einstein 48, 01510 Vitoria-Gasteiz, Spain.

E-mail: [jajuria@cicenergigune.com](mailto:jajuria@cicenergigune.com)

Dr. Laura Oca

Current Address: Mondragon Unibertsitatea, Electronic and computing department, Loramendi 4, 20500 Arrasate/Mondragón, Spain.

Mr. Iñigo Gandiaga

Ikerlan Technology Research Centre, Basque Research and Technology Alliance (BRTA). Pº J.M. Arizmendiarieta 2, 20500 Arrasate/Mondragón, Spain.

**Keywords:** lithium-ion capacitor; metrics; guideline; electric double layer capacitor; mass balance; pre-lithiation; electrochemical energy storage

### Abstract

The fast growth experienced by the field of lithium-ion capacitors (LICs) in the last *quinquennium* led to tremendous progress of this technology. However, the authors observed some parallelism with its Ultracapacitor (UC) sister technology, where an over-rapid growth in the last decade inferred a loss of focus and the need of several tutorials for reconducting incorrect reporting habits. In the light of what is coming, the authors aim to set this work as a direction to the scientific community and the new researchers in the field to serve as i) a retrospective analysis of the original target for LICs to prevent focus deviation, and ii) a guideline for proper LIC design and assembly towards high energy, high power and long cycle life, as well as for a correct electrochemical characterization and reporting. The underlying

thread throughout this report will be the technology behind the frontrunner LIC ULTIMO<sup>®</sup>, a reference device in the market that presents 3-4 times the energy density of an UC and can stand over 1 million cycles, unraveled by means of ante-mortem analysis.

## 1. Introduction

Electrochemical energy storage (EES) is a fast-growing and a fast-moving scenario where new characters are gaining momentum. Historically, batteries have been -and they still are- the system of choice for most energy requiring systems. However, the growing demand of power applications and the development of high energy electrochemical capacitors -also known by the product names of Supercapacitors (SCs) and Ultracapacitors (UCs)- in the mid 90's, set the technology in the EES scenario in early 2000s, with a boom of companies that started to place different products in the market.<sup>[1-7]</sup> However, the non-compliance of market expectations by the end of 2010 together with the consequences of a global financial crisis led to a turbulent period with a redeployment of the main characters.<sup>[8]</sup> Fortunately, it seems that the UC business is now solid, with great market expectations in key economic sectors such as transportation, renewables or electronics (see **Figure 1a**). Parallel to industry, academic research in the field experienced a rapid growth as indicated by the steady increase in the number of annual publications (see **Figure 1b**). In the first period of the century, the growth was contended, and there were several reports devoted to the metrics and the proper characterization of materials and devices given the evolution of the learning curve.<sup>[9-12]</sup> 2010 became a turning point, when the chaos generated in literature by the many novel materials and architectures rising without a universally accepted definition, tremendously difficult to track technology progress. That same year, Conte proposed the actual naming criterion in order to organize the field.<sup>[13]</sup> Soon after, the community experienced an over-rapid growth which required several tutorials in order to “refresh” best practices for measuring and reporting metrics such as capacitance, capacity, coulombic and energy efficiencies, electrochemical impedance, and energy and power densities of faradaic, capacitive and pseudocapacitive materials for supercapacitors. Prof. Simon and Prof. Gogotsi started a cycle of guidance articles in 2011 who themselves closed in 2019,<sup>[14,15]</sup> with many more parallel guidelines been published during those years,<sup>[16-18]</sup> and still seem not to be enough further in 2020.<sup>[19]</sup>

Research in UCs has been driven by the dire need of increasing energy density, the final judge, even for most high-power applications. In 2001, a novel technology emerged to complete the current EES systems trio. Lithium-ion capacitors (LICs) were born in order to fill the energy

gap between batteries and UCs<sup>[20,21]</sup> (**Figure 1c**). LICs are combining both battery and UC characteristics and are rising steeply in academic research since the market uptake by JM Energy -now Musashi Energy Solutions- in 2008 in order to cover applications such as energy regeneration and power assist in automation, backup for emergency power generation or leveling of electric power for renewables. A clear parallelism with its sister technology can be observed, with a first 10-15 years period of contended growth -both industrial and academic-, with some reports attending to the lessons learned.<sup>[12,22]</sup> The rapid growth of academic research observed in the last 5-year period is mainly based on pseudocapacitive, ultrafast faradaic, graphene composites, alloying compounds and many other materials that have found a niche for publication in this technology, based on their fast rate capabilities, and which have already required several yearly review papers to track cutting-edge advances in the field.<sup>[23-27]</sup> Beyond the reviews, which exponentially have grown during the lockdown periods of this pandemic era, authors also observe the need to refresh the technology focus of LICs. In the early years, target was to increase energy, but maintaining as most power and most cycle life as possible from the origin: the UCs. At present, it has become a fierce race towards energy, while power and cycle life have been relegated, getting less and less prominence, to the point that often, only “bad” batteries (low energy batteries) are reported. This is understandable from the point of view that Mathis et al. already raised: “*the current state of the field (referring to EES) nearly requires record breaking performance for publication in high-impact journals*”.<sup>[15]</sup> Despite the already published tutorials with regard to reporting metrics being pertinent for LICs, it is not the only gap that needs to be addressed for this technology in particular. The compelling need of increasing energy also led to inappropriate strategies for device assembly; such as overestimated mass ratios or too wide operating cell voltages, all focused on the increase of energy. Unfortunately, at the expenses of power and cycle life. Surprisingly, plenty of these low energy batteries find their way as LICs in literature, just because they present improved energy over UCs. In order to avoid this practice in the future, the authors believe that i) a retrospective analysis of the original target for LICs to avoid losing focus, and ii) a guide on proper LIC assembly, electrochemical characterization and reporting towards a balanced device with high energy, high power and long durability are still necessary. In view of the rapid increase in academic research and technology progress as well as market uptake expectations for the 2020-2030 period, this report is set as a guideline for the proper design, assembly and characterization of LICs, driven by ante-mortem analysis of the market reference device, LIC ULTIMO®, in order to secure a fast and correct evolution of the technology.

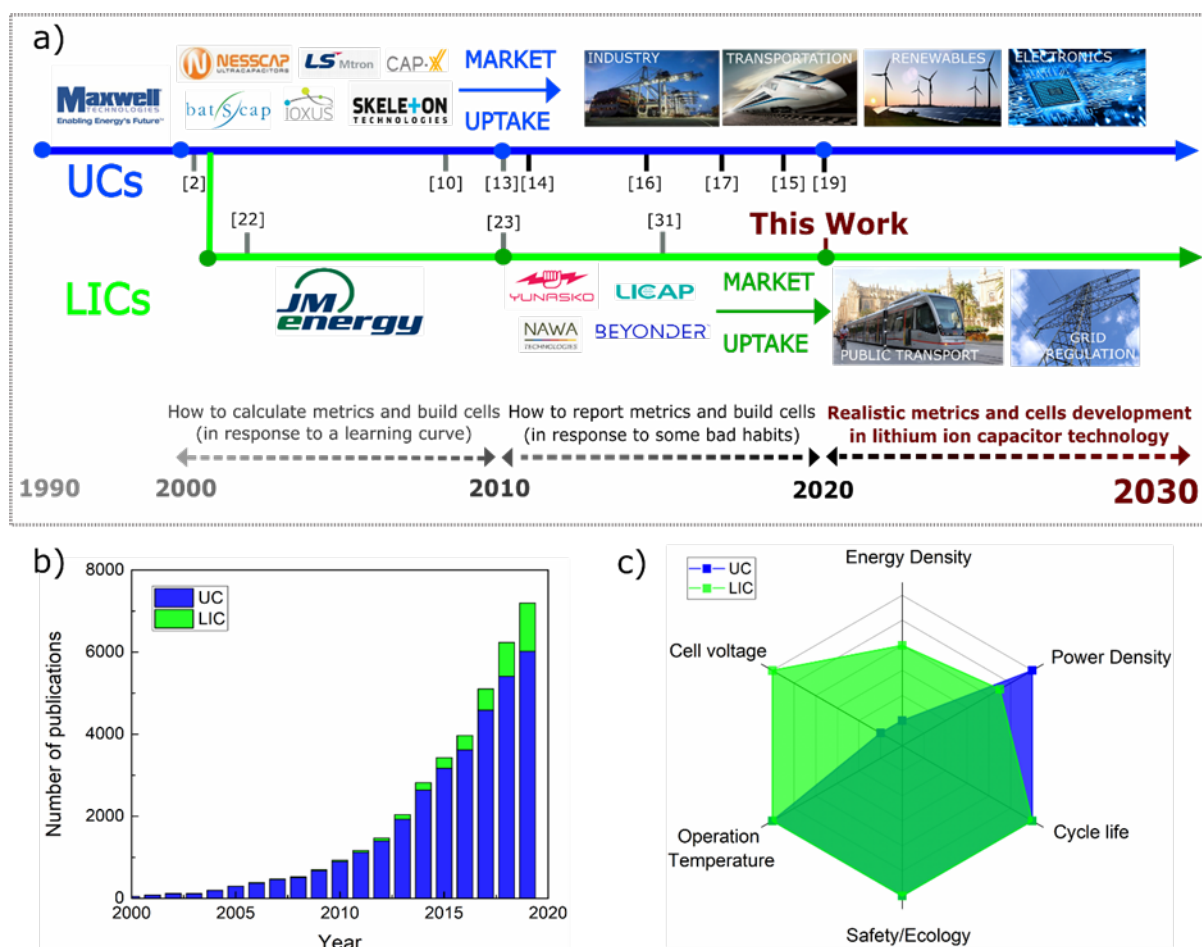


**Figure 1.** a) History is repeating itself: LIC technology follows the same trends as UC technology did both in industry and academia with a ca. 10-year offset. In industry, Maxwell and JM Energy were pioneering their respective technologies, while a period of almost 10 year was needed for the competence to stablish in the market. In academics, the over-rapid growth of the field transformed initial guidelines for reporting metrics and cell assembly in response to a learning curve onto guidelines for proper reporting and correcting questionable habits (see references, colors -grey, black and red- are indicative for their purpose and timeline period they belong). b) Contended growth in academic research for UC and LIC technologies in the first decade while skyrocketing in the second. c) UCs offer high power and cycle life while they are limited in operation voltage and energy density. LICs were born to provide higher voltage and energy density with a minimum lose in power and cycle life.

## 2. Unraveling LIC ULTIMO® design by ante-mortem analysis

ULTIMO® is a registered trademark by Musashi Energy Solutions, founded in 2007 in order to develop, manufacture, and sale LICs, who launched first prismatic LIC in the world already in 2011 and have become the flagship product of the technology over the years. Despite the

difficulty of placing a new technology-based product on such a competitive market as electrochemical energy storage (EES), LIC ULTIMO<sup>®</sup> succeeded on entering several markets segments, such as energy regeneration and assistance in transportation, short power failure backups or energy leveling in renewables and grids. Along these years, LIC ULTIMO<sup>®</sup> has been externally validated (see **Table S1** and **Figures S1-S2**), tested and studied, and performance metrics compared to other UCs.<sup>[28,29]</sup> However, despite some information leaked out, internal device design has been kept under rigorous industrial secrecy and just to name some examples, pre-lithiation process, electrode configuration, mass loading or mass ratios are a mystery to the vast majority of scientist in the field. In order to foster research and shine some light upon proper LIC design, assembly, as well as electrochemical characterization, Musashi Energy Solutions gave CIC energiGUNE permission to carry out an ante-mortem analysis to its 2300 F device (see **Table S1**) and disclose part of the information to the scientific community to conduct this guideline while part is still kept under industrial secrecy to protect their own technology against competitors.

Opening and first visual inspection is in detail provided in **Figure S3**. Physical characteristics of the product and all cell constituents were further characterized with several analytical techniques despite they necessarily need to be kept under industrial secrecy. Briefly, **Figure 2a** illustrates the cell inner configuration and **Figure 2b** shows a selection of pictures taken during the opening process. As observed, the separator and electrodes were still wet from the electrolyte, which allowed for a neat separation of all components, their weighing, and determination of the percentage by weight with respect to the total cell. It can be said that the sum of both electrodes, considering the active (graphite and activated carbon) and the inactive materials (conductive carbon and binder) accounts for a total of 25 % (weight basis) of the prismatic cell (see **Figure 2c**). Thus, similar to UCs, LIC technology can keep a factor of 4 when correlating electrode mass to total mass. Finally, based on the weight of several electrode pieces, with and without coating, it is confirmed that the mass loading of the negative electrode is much lower than that used for batteries, as it is adapted to the needs of high power performance, while the ratio of active material between the positive and negative electrodes is defined to make a contained use of the State of Charge (SoC) of graphite, still being the activated carbon the most abundant material, in order to ensure long cyclability.

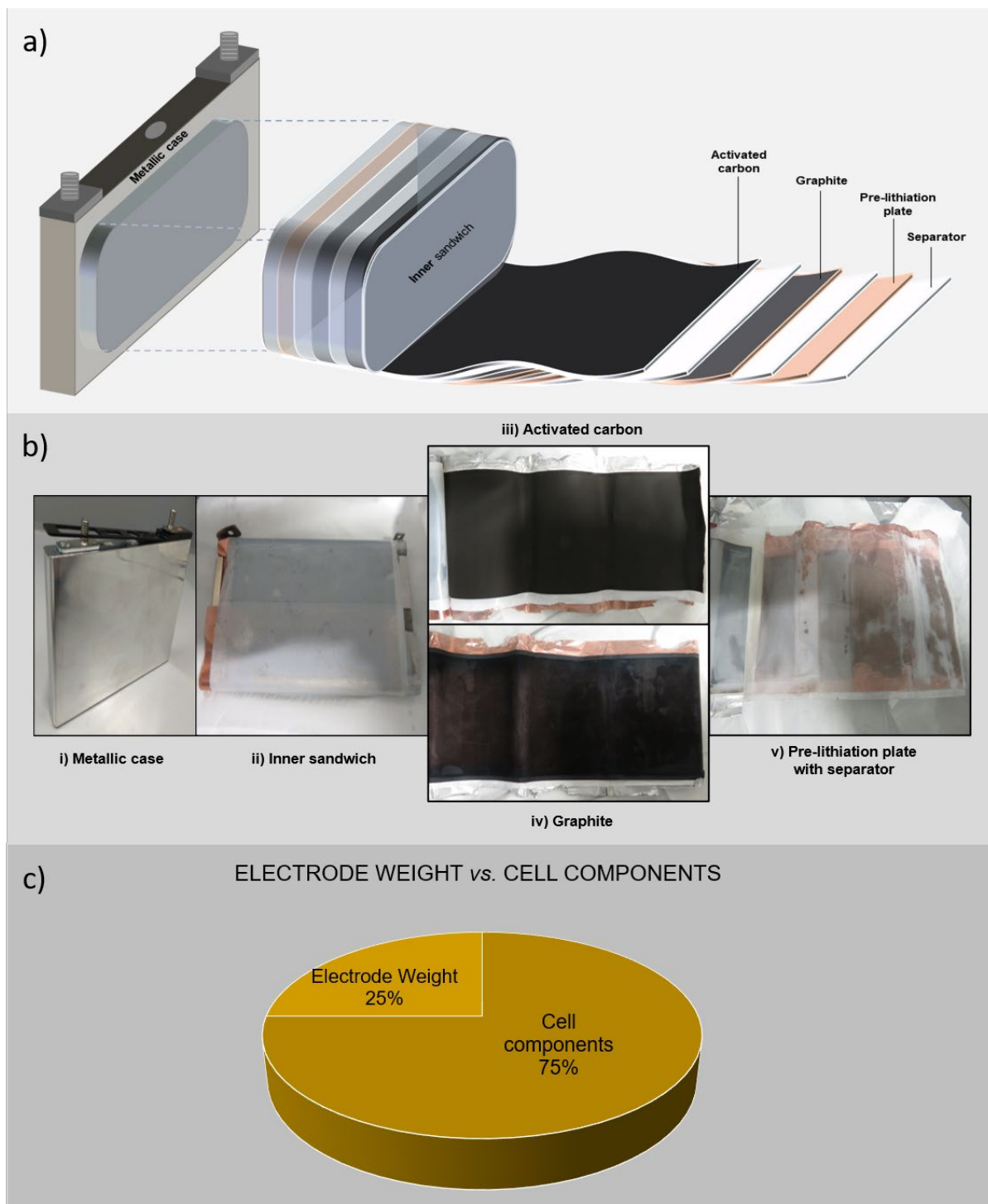


**Figure 2.** a) Illustration and b) image selection of the 2300 F LIC ULTIMO<sup>®</sup> device and its inner cell configuration and constituents: i) metallic case, ii) inner sandwich, iii) positive electrode (graphite, with copper current collector), iv) negative electrode (activated carbon, with aluminum current collector), and v) pre-lithiation plate with separator. c) Contribution in weight (%) of electrode materials respect the overall device weight.

Both electrodes are double-coated as it is observed in the cross-sections under the scanning electron microscope (see **Figure 3**). The positive electrode (**Figure 3** left) is composed of aluminum current collector coated with activated carbon as active material, while the negative electrode (**Figure 3** right) is composed of copper current collector coated with graphite as active material. Electrodes show a compact structure; no detachment of the active material is observed during disassembling, no fractures, marks or defects are found on their surface, and a good cohesion between particles and good adhesion between the current collectors and carbons is observed. With regard to the current collectors, the aluminum shows a chemically etched surface to improve adhesion and minimize resistance while the copper collector has evenly distributed holes (pore diameter of around  $80\ \mu\text{m}$ ) throughout the surface. The presence of these holes allows for the pre-lithiation of graphite, a process that consists on doping graphite with an extra source of lithium ions in order to compensate for the first cycle irreversibility and ensures higher charge-discharge efficiencies. In fact, this approach enables the technology development at industrial scale by pre-lithiating the graphite in a constructed laminated cell, which is key in the fabrication of LICs.<sup>[30]</sup> To that aim, the pre-lithiation plate is used (see **Figure 2b**), which is coated with metallic lithium that diffuses through the graphite in the first charge. The pre-lithiation plate can be observed in detail by SEM in **Figure S4**. It shows a porosity of 30 % which was estimated from SEM images. Further details on the separator and the electrolyte are provided in **Figure S5** and **S6**.

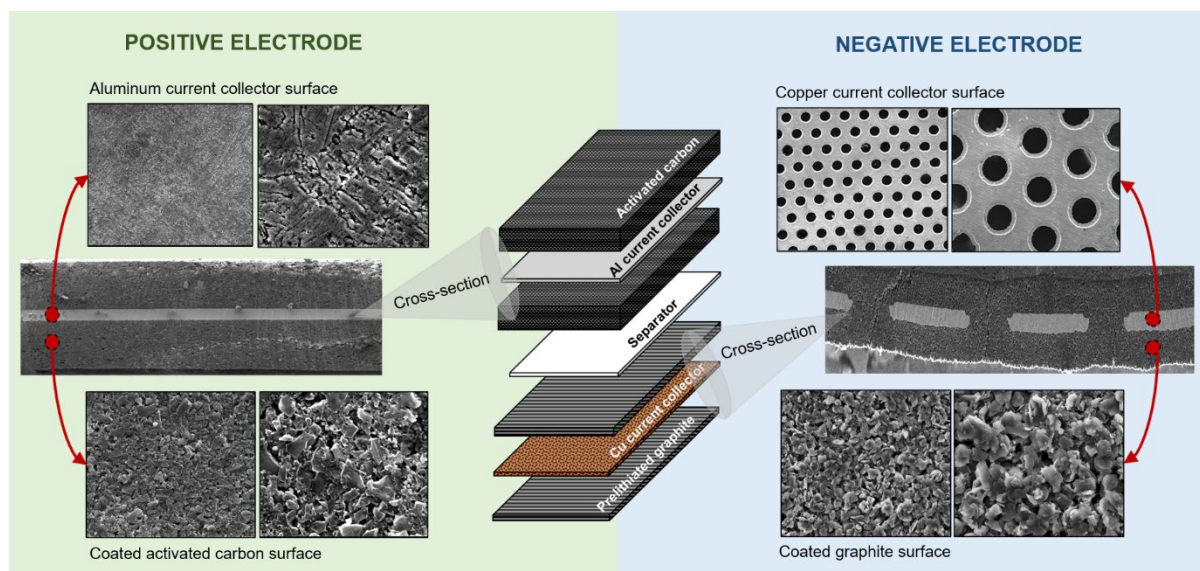


**Figure 3.** SEM images of the positive (left) and negative (right) electrodes in 2300 F LIC ULTIMO®. The cross-section images of each electrode are shown, as well as the top view.



### 3. Guideline for proper assembly, characterization, and reporting of a LIC

Based on the followed ante-mortem study and posterior re-assembly and electrochemical characterization of LIC ULTIMO<sup>®</sup> electrodes, the following lines aim to provide direction on the design concepts as well as on the minimum reporting metrics that are a threshold requirement for proper evaluation of the materials and their potential use in this technology from a purely electrochemical point of view. Being numeric values irrelevant to carry out this exercise, they are kept unrevealed to avoid industrial benchmarking. **Figure 4** shows a scheme where it is indicated how electrode materials should be characterized in 3 electrode cells by means of cyclic voltammetry (CV), galvanostatic charge/discharge (GCD) and electrochemical impedance spectroscopy (EIS), and reporting metrics should be rather in terms of capacity or capacitance depending on the nature of the material. One of the most important outcomes of this preliminary characterizations needs to be an optimum mass ratio between negative and positive electrodes towards the fabrication of a well equilibrated LIC in terms of energy, power and cycle life. That LIC can be characterized in a 2-electrode set-up by means of GCD and EIS to define the internal resistance, the capacity (or capacitance) and capacity retention over different discharge times, the energy-to-power ratios as well as the energy efficiency and the stability.

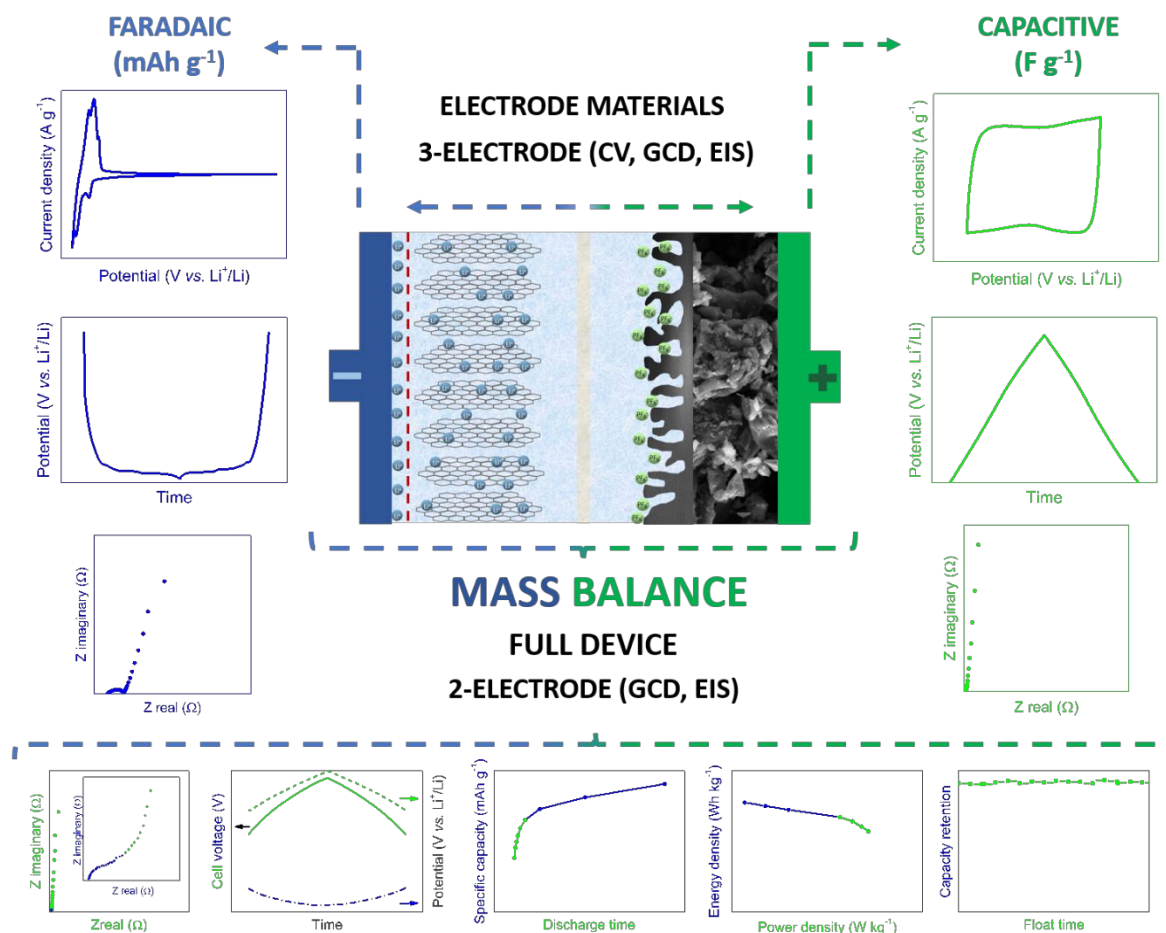


**Figure 4.** Electrochemical threshold characterization requirements towards optimum design, assembly and characterization of electrode materials and LICs. Blue color represents LIC characteristics ascribed to the faradaic electrode, which are cell voltage, high specific capacity and high energy. Green color represents features attributed to the capacitive electrode, which are cell voltage profile, fast discharge time, high power density and long cyclability.

Much has been written about reporting metrics of different type of materials, but very little on the proper design, characterization and reporting of LICs. Thus, the next sections of the article are organized as follows: i) electrochemical evaluation of electrodes with key aspects and methods to categorize materials, based on ULTIMO<sup>®</sup>'s graphite and AC electrodes and described in **Figures 5 to 9** and **Tables S2** and **S3**, ii) LIC design and assembly is discussed below, with focus on two critical factors that determine the overall performance of LICs: mass ratio and pre-lithiation, and iii) electrochemical evaluation and reporting of LICs is addressed in terms of their main performance indicators.

### 3.1. Electrochemical evaluation of materials

First of all, electrochemical characterization of the materials should be better done in a 3-electrode set-up rather than in 2-electrode, using two different metallic lithium discs as counter and reference electrodes. Furthermore, in the case of activated carbon (AC) -or any other capacitive material- it is interesting to use an oversized AC counter electrode in order to avoid any polarization at high rates, especially if beyond LIC technologies are studied.<sup>[31,32]</sup> Second, measurements of basically voltage, current and time should be followed by using cyclic voltammetry (CV), galvanostatic charge-discharge (GCD) and electrochemical impedance spectroscopy (EIS) to provide minimum key parameters such as operating potential window, capacity/capacitance and rate capability, coulombic efficiency, internal resistance and cycling stability of materials in the way it is done from **Figure 5** to **9**. Finally, the use of integration formulas for LICs is strictly necessary since charge storage usually differs from that of purely capacitive materials and devices (**Tables S2** and **S3**).

### 3.1.1. Operational potential window

Cyclic Voltammetry is used to qualitatively analyse materials, in order to establish the operational potential window, identify what type of charge storage mechanisms take place and at which potential. In this case, being both materials well-known, only a representative voltammogram is shown in **Figure 5a** and **5b**. CVs are usually recorded at very low scan rates -typically between 0.1 to 1 mV s<sup>-1</sup>- for faradaic materials in order to ensure that all redox reactions occur completely. In this case, graphite was characterized at a scan rate of 0.1 mV s<sup>-1</sup> showing a narrow voltammogram from open circuit potential (OCP) until 0.3 V vs. Li/Li<sup>+</sup> where Li<sup>+</sup> insertion in between graphene layer starts occurring (see **Figure 5a**). Since the pre-lithiation step is carried out in factory, no solid electrolyte interface (SEI) formation is observed in this case. Capacitive materials such as AC stores charges by physisorption of ions onto the surface, enabling very fast ad/desorption of species. Thus, faster scan rates are possible, even necessary to avoid parasitic redox reaction occurring in the surface of the materials at low scan rates. Classically, 5 or 10 mV s<sup>-1</sup> is a good starting point. According to its capacitive nature, in **Figure 5b** the AC presents a rectangular voltammogram where the output current is constant and independent to the applied potential, and anions and cations are stored above and below the OCP respectively. In this case, cyclic voltammograms of the most common used potential window (*i.e.* 2 – 4.2 V vs. Li<sup>+</sup>/Li) and the adequate one for this device (*i.e.* 2.2 – 3.8 V vs. Li<sup>+</sup>/Li) are shown to demonstrate its undoubtedly capacitive behaviour at both potential windows.

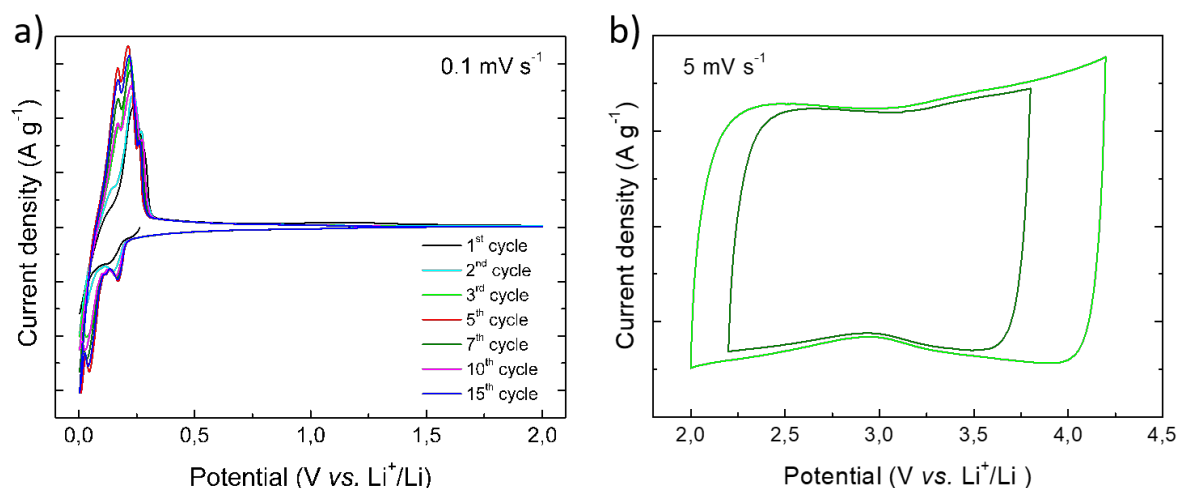


**Figure 5.** Cyclic voltammograms: a) Graphite at 0.1 mV s<sup>-1</sup> and b) Activated carbon at 5 mV s<sup>-1</sup>.

Determination of the safe potential window in positive electrodes is typically done by incremental potential steps of  $\pm 0.2$  V starting from the OCP to the point where an exponential increase of the current response is observed and Coulombic Efficiency (CE) goes below 99 % (see **Figure 6a**). Meanwhile, cyclic voltammetry at faster scan rates can give an idea about its behaviour at high currents (see **Figure 6b**), showing undistorted quadratic shape when low resistance and showing tilted curves at the corners when increased resistance.

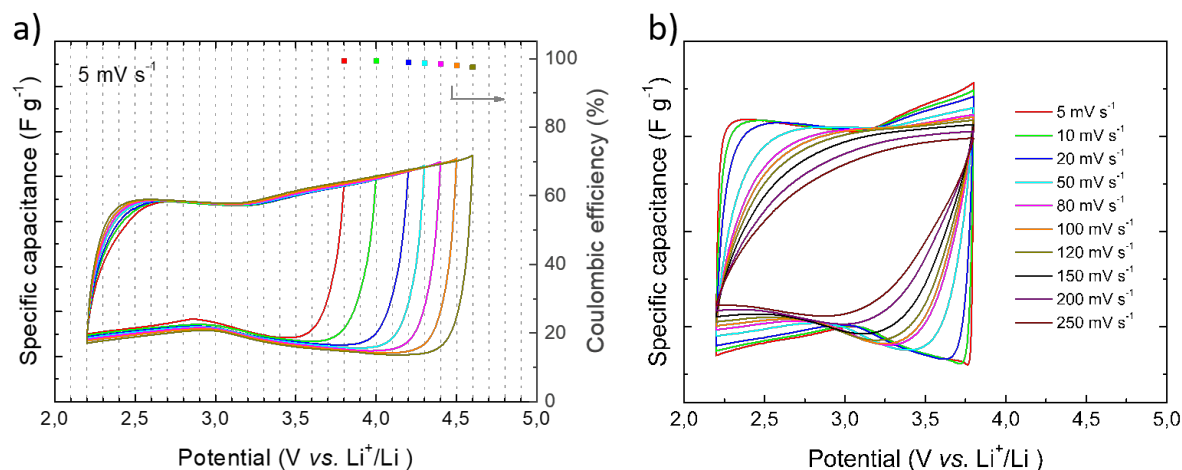


**Figure 6.** Cyclic voltammetry of Activated Carbon: a) determination of the upper potential and b) different scan rates evaluation.

### 3.1.2. Capacity, capacitance, rate capability and coulombic efficiency

Galvanostatic charge-discharge (GCD) is carried out to quantitatively characterize the charge storage capability of the materials, usually within the potential range established by CV analysis. **Figure 7** shows potential vs. capacity profiles for both materials at different applied current densities. **Figure 7a** shows GCD profile of graphite, showing a large plateau below 0.2 V vs.  $\text{Li}^+/\text{Li}$ , in good agreement with the redox peak observed in the voltammogram graph (see **Figure 5a**). **Figure 7b** shows symmetrical GCD profile, which is characteristic of capacitive materials.

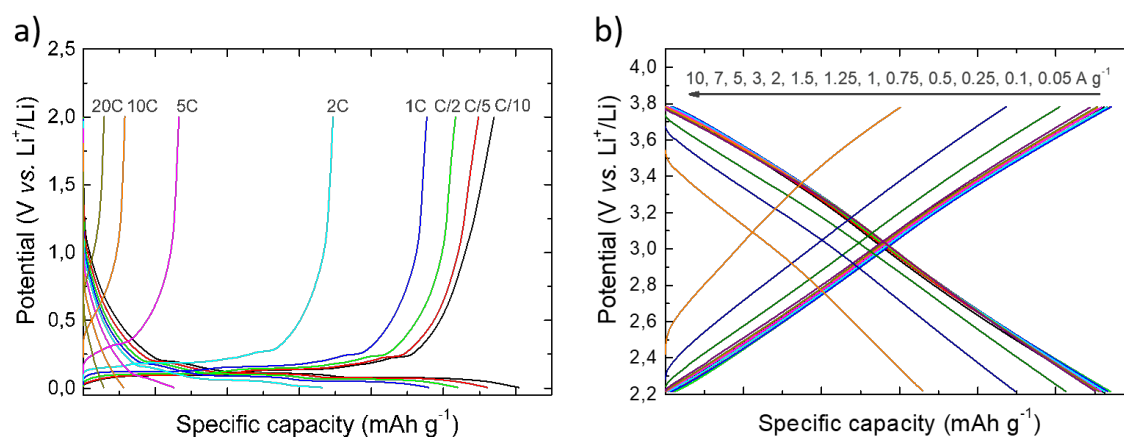


**Figure 7.** Galvanostatic charge-discharge profiles of a) Graphite between 0.005 – 2 V vs.  $\text{Li}^+/\text{Li}$  and b) Activated carbon between 2.2 – 3.8 V vs.  $\text{Li}^+/\text{Li}$ .

In order to set the rate capability properties, *i.e.* how much capacity the electrode can retain as the current density increases, increasing current densities are applied. Faradaic materials are usually discharged at constant current (CC), while charged at constant current constant voltage mode (CCCV), an initial CC charge up to a specific voltage aided with a final constant voltage step. The rate capability properties of batteries are usually analysed at different C-rates, typically from C/20 to 1C or 2C maximum, where C is the theoretical capacity of the studied material. Considering the particular characteristics of LICs, which are aimed to operate at fast charge and discharge rates, the constant voltage step is suppressed and the testing range is extended to higher C-rates to evaluate power capabilities. Moreover, in the case of battery-type materials, an additional upper x-axis with the equivalent current density to aid comparison with the capacitive electrode material will be very helpful (see **Figure 8a**). Materials with better rate capabilities will endow devices with higher energy and power densities. However, in addition to rate capability data, coulombic efficiency of the materials, *i.e.* the ratio of extracted charge during the discharge step to the stored charge during charging needs to be reported. Coulombic

efficiency (CE) below 100% implies loss of charge due to irreversible reactions, series resistance or leakage current which turns out in heat dissipation, reducing cycle life. Thus, understanding the origin behind the CE loss is key to develop a long-lasting system. **Figure 8a** and **8b** show rate capability of graphite and AC. Graphite performance varies considerably upon characterization method. Under CCCV it presents outstanding rate capability performance, with no impact on CE up to 20C, however, performance differs considerably when potentiostatic step is removed. It needs to be considered that LICs will predominantly perform under constant current only. The GCD measurements of the AC were followed in two different potential windows, 2.2 – 3.8 V and 2 – 4.2 V vs. Li<sup>+</sup>/Li. This way, we can see that enlarging the potential window of the AC will of course give higher capacity values, but it could not well adjust to the real behaviour of the final device. Thus, the most correct potential window, which in the case of graphite-based LICs is normally the same as for the final device (*i.e.* 2.2 – 3.8 V vs. Li<sup>+</sup>/Li), should be selected for posterior correct mass balancing of the electrodes. As shown in **Figure 8b** the specific capacity values are maintained almost constant in the current density range up to 2 A g<sup>-1</sup>, while at higher current densities it smoothly decreases. However, still the ca. 78 % of capacity is retained in the studied current density range. Capacity values, instead of capacitance values, should be given for the posterior mass balancing between faradic and capacitive electrodes.

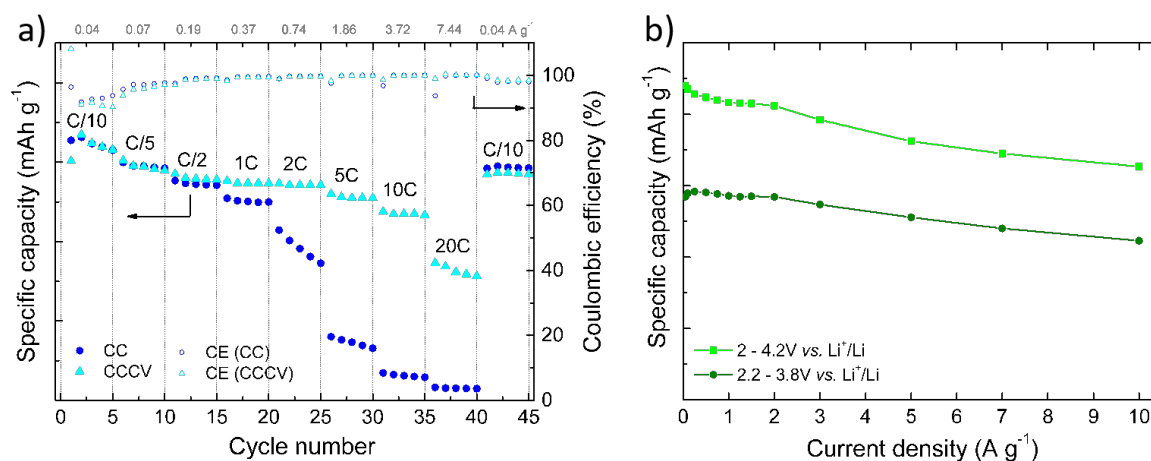


**Figure 8.** a) Rate capability of Graphite between 0.005 V – 2 V vs. Li<sup>+</sup>/Li at constant current (CC) and constant current with constant voltage (CCCV) step and b) Specific capacity values of AC between 2.2 – 3.8 V and 2 – 4.2 V vs. Li<sup>+</sup>/Li at different current densities.

### 3.1.3. Equivalent series resistance and cycle life

Equivalent series resistance (ESR) accounts for the sum of the resistances of the bulk electrolyte resistance, contact resistance of the electrode and the current collector as well as the resistance of the material. Despite it can be calculated from the CV and the GCD, it can be done more accurately by electrochemical impedance spectroscopy. Electrochemical impedance spectroscopy allows obtaining the electrical impedance as a function of the applied electrical current frequency. With this technique, capacity/capacitance as well as ESR or charge storage mechanism can also be analysed. Nevertheless, data analysis is not straightforward since the experimental data needs to be fitted to an equivalent circuit. Thus, qualitative analysis is typically reported in literature. To this aim, Nyquist plots need to be represented in a one-to-one ratio, x-y axis forming a square. The impedance intersection with the x-axis will give the quantitative value of the ESR. Posterior semicircle and 45° and 90° lines will provide information on the charge transport and diffusion through the electrodes. In the case of LIC ULTIMO<sup>®</sup>, both graphite and AC present very low ESR, representative of the good engineering of the electrodes.

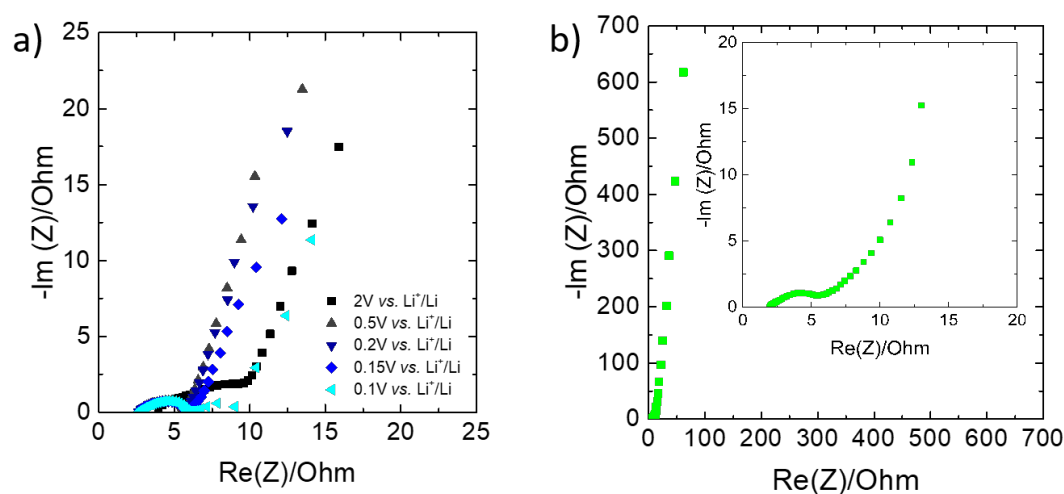


**Figure 9.** Electrochemical Impedance Spectroscopy at different potentials for a) Graphite and at the OCP for b) Activated Carbon.

### 3.2. LIC design and assembly

The following steps prior to LIC assembly are the most critical and will determine the overall performance of the final LIC device: mass ratio ( $m_+ \cdot C_+ \cdot \Delta V_+ = m_- \cdot C_- \cdot \Delta V_-$ ) and pre-lithiation. Anytime a LIC is assembled, characterized and reported, such matters need to be addressed. It is worth to highlight that classical mass balancing applied for LIBs is not valid anymore for

LICs. With regard to the pre-lithiation, if not tackled and electrochemical pre-lithiation is used,<sup>[33]</sup> at least a short overview in the introduction is deserved. In the following lines, these two steps are more thoroughly explained.

### 3.2.1. Mass ratio

In order to set a correct electrode mass ratio between the negative and positive electrode active mass loadings and ensure a well-balanced LIC in terms of energy, power and cycle life, a different strategy to that used in batteries is necessary. LICs cannot be balanced on the basis of making full use of the charge stored on the negative electrode since power and lifetime will be severely affected. Furthermore, it is neither suitable to set a mass ratio based on capacities obtained at low C-rates if the full cell targets high currents and short discharge times. Thus, in order to set a correct criterion, capacity of both materials respect to current density should be represented first (see **Figure 10a**). Now, electrode mass balancing needs to be accurately defined in order to develop an equilibrated system. If mass ratio is maximized, *i.e.* large SoC-window of negative electrode is used, very high energies will be achieved, since the extended use of the anode will allow to increase the mass of the AC, which is the energy limiting factor. However, this will limit power owing to the sluggish kinetics of the anode, and accelerate degradation. If the mass ratio is too low, *i.e.* low SoC-window of negative is used, power and cycle life will be excellent, but lack of energy will be considerable too. Thus, the optimum ratio, where the anode is used to an extent where high energy densities are obtained, keeping high power and without compromising cycle life owing to a contended operative SoC of the negative electrode, which is normally between 10 % and 50 %, might vary depending on the final product requirements. Finally, this optimum mass ratio should be defined based on electrode capacity output at high currents, where the LIC targets its operation. Thus, setting the proper mass ratio is not trivial. In fact, it is rather complex and might take some iterations. However, a systematic study might not be needed depending on the type of research, but if reporting a final device, at least the criterion for the selected mass ratio should be well reported.

### 3.2.1. Pre-lithiation

Pre-lithiation is currently the barrier to overcome for market success of this technology and it needs to be addressed both from the scientific point of view but also from the technical implementation side.<sup>[34,35]</sup> Despite the challenge, or maybe, because of the great challenge it represents, very little academic research is focused on the topic. Carbons, the dominant



materials in the field, not being a natural source of lithium, they lack an internal source to compensate for the first cycle irreversibility without depleting the lithium content in the electrolyte, thus compromising performance and cycle life. LIC ULTIMO® presents a smart solution based on an additional electrode with the exact content of lithium. This is an extremely important detail<sup>[36,37]</sup> to pre-lithiate all the graphite electrodes in the cell by lithium diffusion through micromachined copper electrodes (see **Figure S4** and **10b**). Nevertheless, the need for metallic lithium is a handicap, given the increase in production cost and the need for safe handling of lithium in an oxygen free atmosphere. Recently, the development of several strategies that are compatible with atmospheric ambient might be the game changer that will trigger the market uptake of the technology.<sup>[38,39]</sup> That said, at this point, if the system has an inherent source of lithium to compensate for the first irreversible cycle, the system is ready for characterization. Otherwise, electrochemical pre-lithiation should be carried out first.<sup>[33]</sup>

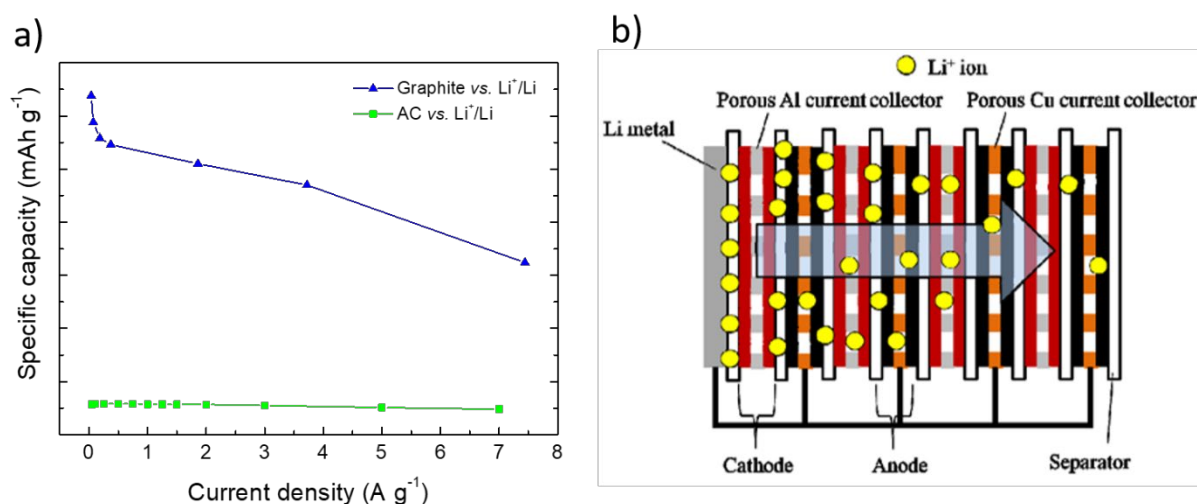


**Figure 10.** a) Mass ratio selection: specific capacity values of Graphite and AC vs. Li<sup>+</sup>/Li at different current densities. b) Pre-lithiation strategy adopted by Musashi Energy Solutions [30].

### 3.3. Electrochemical evaluation of LICs

#### 3.3.1. Equivalent series resistance, capacity, capacitance, rate capability and energy efficiency

Electrochemical evaluation of EES systems is usually done by means of cyclic voltammetry (CV), galvanostatic charge-discharge (GCD) and electrochemical impedance spectroscopy (EIS). CV is a powerful analytical tool to characterize materials. It can also give a fast glance of a full cell, especially with regard to determine the limit on the upper voltage. However, real power devices operate under current, thus, GCD is more appropriate to characterize full cells.

Thus, voltage and time should better be measured under varying conditions of current to record charge-discharge profiles and calculate capacity (capacitance could be used if charge-discharge profiles are strictly linear) and rate capability.<sup>[15]</sup> Finally, together with the equivalent series resistance (ESR), the energy efficiency of the device could be established. ESR can be calculated both from CV and GCD measurements, however, a more appropriate technique seems to be EIS, which different to CV and GCD, is performed in steady state conditions. EIS measurement is easy to perform, although its interpretation is far more complex and has been in depth studied in literature. However, it is a fast way to ensure the quality of the assembled device. Typically characterized in the frequency range from 1 MHz to 10 mHz, when represented in a Nyquist Plot, the intersection of the real axis at the highest frequency will be the ESR of the overall system. Characteristically, well-assembled LIC devices should present low ESR values, close to that of supercapacitors, in the range of few m $\Omega$ . Higher values are indicative of non-optimize systems. The signature of the overall spectra is also similar to that of supercapacitors, despite it will always present a small faradaic in origin charge transfer semicircle at the high frequency domain and a slightly tilted capacitive line in the lower one. Nevertheless, depending on the selected materials, EIS spectra, as well as cell performance, can vary substantially.<sup>[40,41]</sup>

Often, LIC charge-discharge profiles ranging from discharge times of thousands of seconds to hundreds of seconds are summarized in a single graph what makes it difficult to extract information about the symmetry and the ESR from the profiles recorded at the fastest discharge times. In addition, considering that LICs are power focused devices, their limits should be challenged, and so, be charge-discharged even in few seconds. In fact, showing symmetric and ideal profiles at discharge times of several minutes is not worth if real life applications are in the range of seconds. Furthermore, the use of a reference electrode to characterize a novel system is strongly recommended in order to monitor the potential swing of both electrodes at different current rates, from several minutes to few seconds (see **Figure 11**). Note that to perform this experiment correctly, capacitive electrodes need of some time for charge redistribution, thus a voltage hold of minimum 6 times the time constant ( $\tau$ ) of the equivalent first-order Thevenin model (*i.e.*, few seconds, 5 s in this case) is necessary between charge and discharge.<sup>[42]</sup> Monitoring the electrodes allows i) observing the performance of each of the electrodes at different operation regimes, ii) evaluating whether the mass ratio is correct or needs to be revised, iii) establishing a safe operating voltage limit to avoid both plating in the negative electrode and electrolyte decomposition in the positive electrode, and iv) predicting, up to an extent, cycle life of the system on the basis of SoC of the negative electrode when the

LIC operates into the limit. If the mass ratio is correct and the materials are fast, sub-minute performance should be easily reached even at lab-scale electrodes, which are not expected to be as well engineered as commercial LIC ULTIMO® electrodes are.<sup>[43–45]</sup> In this case, it can be observed that at discharge times of 40 minutes, 100 s and 30 s the cell voltage profile of the LIC is perfectly symmetric, and the potential swing of the AC remains almost constant, while the lower potential of the graphite moves from 11.6 mV to 6.5 mV and 3.6 mV vs. Li<sup>+</sup>/Li, respectively. Of course, there is a slight increase on the ESR when reducing discharge time from 100 s to 30 s that reduces the energy efficiency (EE) from 98% to 91%, still obtaining very high EE over 90 % for the most stressful condition.

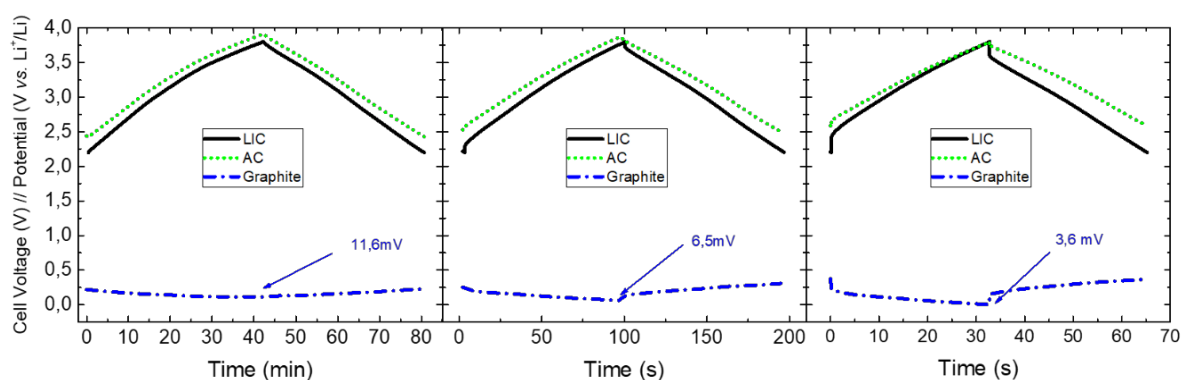


**Figure 11.** Galvanostatic charge-discharge profiles for full LICs (black straight line), positive (AC, green dot line) and negative (graphite, blue dash-dot line) electrodes at different discharge times from several minutes to few seconds measured at room temperature (*i.e.* 25°C).

In order to get the whole spectrum, a capacity (or capacitance if applicable, or even better, both) vs. discharge time (or current density) is very useful, showing only operative discharge times or otherwise identifying the points in which plating occurs. In **Figure 12a** capacity retention over discharge time can be observed.

### 3.3.2. Energy-to-power density

When it comes to full devices and technologies, energy-to-power ratio is considered to be the main characteristic for evaluation and comparison, usually done by using Ragone plot, which has become a rather controversial graphic in academic research, owing to the next three questions briefly analysed below:

- i) *Energy-to-power reported respect to which mass?*

It is widely accepted in academia that Ragone plots should be reported respect to the total active mass of both electrodes. However, it is very important to try to report results in such a way that extrapolation to a real device is as straightforward as possible. Thus, Ragone plots should rather be referred to the total mass of the electrodes to avoid favouring formulations (*e.g.* typically 80:10:10) containing high loadings of conducting carbon and binders, which are unrealistic in real devices and might overestimate material performance. A rather controversial point is also the mass loading. Low loadings ranging from *ca.* 1 to 5 mg cm<sup>-2</sup> are deemed to be unrealistic in real life, based on previous knowledge from battery and UC technologies, were usually a loading threshold of 5 to 10 mg cm<sup>-2</sup> is considered.<sup>[14,46]</sup> Yet, LIC is a different technology, with a set of performance assets that clearly differentiates from batteries and UCs, what definitively implies a different design, as demonstrated herein. This work serves to proof that commercial LICs operate with low mass anode loadings compared to LIBs and UCs, and still the correction factor to the real device is similar to that for UCs and LIBs, established to be 25 % for this prismatic device (see **Figure 2c**). As it can be seen in **Figure 12b**, there is no need to obtain outstanding energies based on electrode weight to reach the market, but it needs to be well balanced together with a certain number of techno-economical properties. Finally, it is worth remembering that real applications are mostly conditioned by volumetric restrictions; thus, volumetric performance is more relevant than the widespread gravimetric performance. This, needs to specially be considered when devices are build based on low density materials.

ii) *Energy-to-power calculated, how?*

In academic research energy and power are usually calculated from the voltage and time measured by characterizing the system under different current conditions at a certain operative cell voltage. Three issues arise herein: the extension of the applied current, the operative voltage window and whether energy should be calculated from an applied constant current or a constant power. The applied current should allow to discharge the LIC within the range where batteries operate, from 1 hour to 10 minutes, as well as within the range where UCs work, from 10 min to 1 s or at least down to the fastest discharge time prior unsafe operation occurs. Second matter has not got a straightforward answer, it is responsibility of the researchers to choose realistic cell voltage, without exceeding neither the upper nor the lower limits for the sake of energy at the cost of safety and cycle life. Thus, the selected cell voltage should be endorsed by long cyclability or float time. Third matter seems to be opting for constant power, as supported by relevant figures in the field<sup>[47]</sup>. However, assuming most reported devices will never go beyond

the lab, not to say cross the market barrier, calculating energy from current is a suitable method, but it should be done by integrating the area below the voltage vs. time graphic in order to avoid under/overestimation than that induced by the characterization method.<sup>[18]</sup>

iii) *Energy-to-power compared to what?*

Ragone plot has become a tool to highlight one system over the rest. Apart from many other reasons, such as fair comparisons are almost impossible since device designs, optimization degree and characterization conditions differ considerably from each other, the major reason is that it is unrealistic to try to highlight that a material is better than others by evaluating the energy-to-power characteristics of a lab-scale device. Simply because there is an eternity from a lab device to an industrial product. Thus, the authors strongly recommend to avoid comparative Ragone plots, especially those aimed at showing that one device is better than the rest.

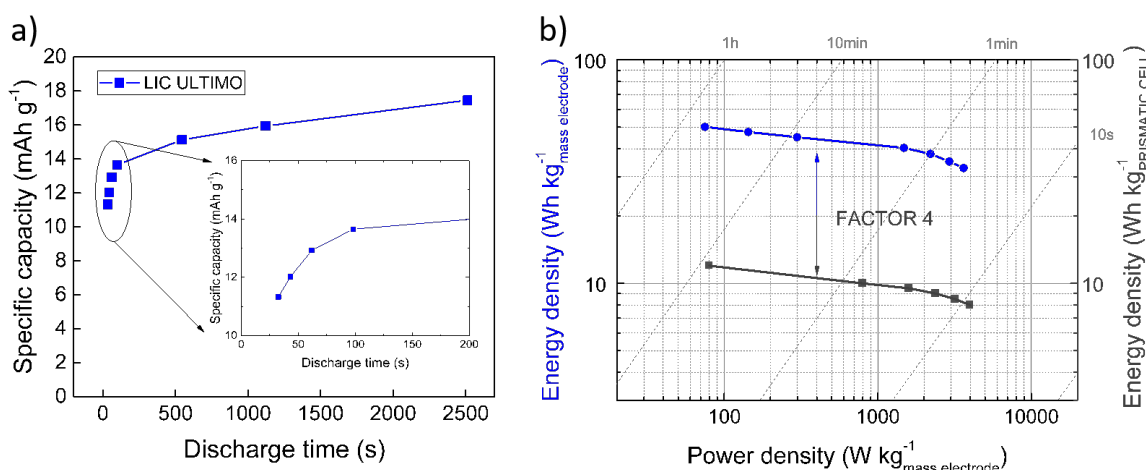


**Figure 12.** a) Charge storage capabilities (specific capacity) as a function of the discharge time, b) Ragone Plot showing energy-to-power ratios of LIC ULTIMO<sup>®</sup> based on the weight of two electrodes (blue) and the full device (black), with a correction factor of 4.

### 3.3.3. Cycle life, float time, self-discharge

Finally, a full device cannot be reported without providing cycle life information. Especially for those materials presenting considerably large volume expansions, cycle life tests should be reported since it is a major go/no-go criterion. Usually cyclability tests are reported, but the long duration of these tests (up to 3 years in this case, see analysis in **Figure S2**) and the lack of a standard protocol makes comparatives difficult. Accelerated ageing can be reported based

on floating tests, by holding cell voltage at the upper limit and evaluating capacity fade and impedance every certain number of floating hours. Despite industrial requirements demand floating tests to be conducted at high temperature (*i.e.* 60 - 70 °C), that should be done under strict safety conditions that might not be available in academic centres, where floating at room temperature should be valid. End of life is considered when the initial capacitance drops over 20 % or the resistance increases by a factor of two. Tests conducted in **Figure 13** for re-assembled LICs show capacitance retention of 80 % after 1000 float hours both at room and high temperature, confirming the robustness of ULTIMO<sup>®</sup> electrodes. In addition, despite not being critical at lab-scale, if an eye is set in a beyond-lab step, self-discharge should also be studied by monitoring voltage decay when the system is left at open circuit voltage (OCV) once it is charged.

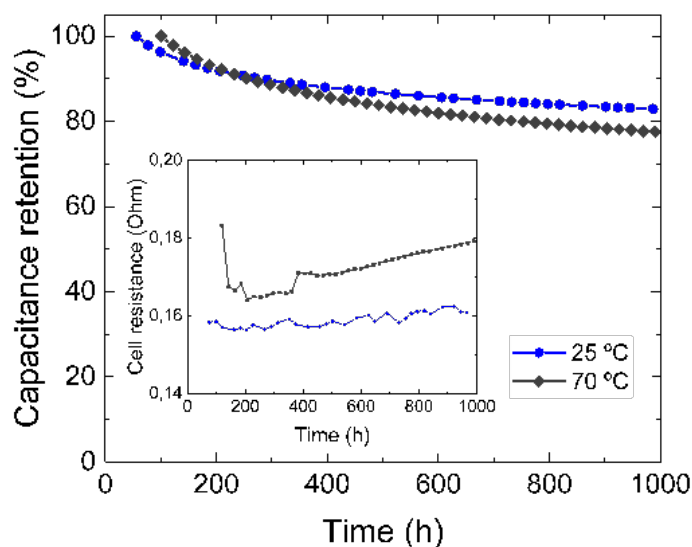


**Figure 13.** Floating test carried out at room temperature (*i.e.* 25 °C) and 70°C to re-assembled LIC ULTIMO<sup>®</sup> devices.

#### 4. Conclusions

Market expectations for LIC technology are very promising for the coming years in view of the already available products, which start to be part of integral solutions, covering a wide range of applications, as well as the increasing number of new firms entering the business. In order to boost academic progress and technology transfer, mistakes from the past need to be avoided by lessons learned in the field of supercapacitors, evading efforts to be diluted in a chaotic panorama of materials, metrics and designs. This way, LIC ULTIMO<sup>®</sup> has been unraveled, with

the aim to provide focus on real aspects and challenges of the technology for the scientific community, and generate a wide-ranging consensus on design and reporting metrics based on the product that has been -and still is- the flagship of the technology for more than a decade. Thus, this work aims to serve as a guideline for proper design, assembly and characterization of LICs, giving evidence of the importance of pre-lithiation, current collectors, electrode designs, separator, electrolyte formulation, mass loading, mass balance, and a correct balance between energy, power and cycle life rather than developing devices that perform outstandingly in terms of energy, but fails on the rest of parameters that are of utmost importance for real technology development.

## 5. Experimental Section/Methods

*Cell assembly and electrochemical characterization:* Punched out electrodes were first cleaned with dimethyl carbonate (DMC) solvent in order to remove the residual salt of the electrolyte and then, characterized as half cells in three-electrode Swagelok® airtight systems using lithium metal disks as reference and counter electrodes. The cells were assembled using the same cellulose separator of LIC ULTIMO®. The electrolyte used was 1 M LiPF<sub>6</sub> in ethylene carbonate (EC), ethylene methyl carbonate (EMC) and dimethyl carbonate (DMC) (1:1:1 in vol., Solvionic). All systems were assembled inside a glove box under argon atmosphere. Cyclic voltammetry (CV), galvanostatic charge/discharge (GCD) and electrochemical impedance spectroscopy (EIS) measurements were recorded with a multichannel potentiostat (Biologic VMP3, France). The electrochemical characterization of graphite was carried out between 0.005 – 2 V vs. Li<sup>+</sup>/Li, while the measurements of AC were followed by different potential windows depending on the interest of the measurement. Final LICs were also assembled in three-electrode Swagelok® airtight systems using a lithium metal disk as reference electrode in order to monitor the behavior of both positive and negative electrodes. LICs were characterized in a cell voltage window of 2.2 – 3.8 V. GCD measurements were followed and recorded for all full cell devices at different current densities. EIS measurements for LICs were conducted using a multichannel VMP3 generator (Biologic VMP3, France) applying a low sinusoidal amplitude alternating voltage of 10 mV over zero current potential (OCP) at frequencies from 1 MHz to 10 mHz.

*Microstructural analysis of electrodes:* Scanning electron microscopy (SEM) was utilized to analyse the microstructural analysis of the surface and cross-section of negative and positive electrodes. Images were acquired with a field emission Thermo Fisher Quanta 200 FEG high-

resolution microscope. Cross-section sample were prepared by a Hitachi 4000 Plus ion milling, which utilizes a broad, low-energy Ar<sup>+</sup> ion beam (0 - 6kV acceleration voltage) milling method.

*Separator characterization:* Fourier-transform infrared (FTIR) spectroscopy was used to determine the composition of the separator. FTIR data were collected in a FTIR Spectrum 400 DTGS (Perkin Elmer).

*Electrolyte composition:* A gas chromatograph (Perkin Elmer, Clarus® 590) coupled to a mass spectrometer (Perkin Elmer, Clarus® SQ 8 T) was used to determine the solvents of the electrolyte. The used column was Elite-35 MS (30 m × 0.25 mm x 0.25 μm) with helium as the carrier gas (column flow of 1 mL min<sup>-1</sup>). Set-up controlling and data analysis was done with the software Turbomass (version 6.1.1), while compounds were identified by their retention times and by matching their mass profile with the NIST MS Search Library (version 2.0). Liquid-state nuclear magnetic resonance (NMR) was used to determine the salt composition of the electrolyte. NMR spectra were collected with Bruker Avance III HD NanoBay spectrometer of 300 MHz, with a 5 mm BBFO probe with gradients. The nuclei under study were <sup>19</sup>F and <sup>31</sup>P and data were analysed with the MestreNova software.

## Supporting Information

Supporting Information is available from the Wiley Online Library or from the author.

## Acknowledgements

The work was financially supported by the Basque Country Government under the Elkartek 18 program (CICe18, KK-2018/00098).

Received: ((will be filled in by the editorial staff))

Revised: ((will be filled in by the editorial staff))

Published online: ((will be filled in by the editorial staff))

## References

[1] “Maxwell Technologies cell product lines Standard Series, XP™ Series, DuraBlue, Pseudocapacitors.,” can be found under <https://www.maxwell.com/products/ultracapacitors/cells>, **1965**.

[2] A. Burke, *Journal of Power Sources* **2000**, *91*, 37.



- [3] “French CleanTech™ | Energy storage,” can be found under <https://www.frenchcleantech.com/company/categories/energy-storage/profile/batscap-lithium-metal-polymer-battery.html>, **2001**.
- [4] “Products | IOXUS - Worldwide Energy Products,” can be found under <https://ioxus.com/english/products/>, **2007**.
- [5] “Products | LS Mtron,” can be found under <http://www.lsmtron.com/page/productMain.asp>, **2008**.
- [6] S. Technologies, “All Products | Skeleton Technologies,” can be found under <https://www.skeletontech.com/all-products>, **2009**.
- [7] CAP-XX, can be found under <https://www.cap-xx.com/>, **1990**.
- [8] “Supercapacitor / Ultracapacitor Interviews, Strategies, Road Map 2015-2025: IDTechEx” can be found under <https://www.idtechex.com/en/research-report/supercapacitor-ultracapacitor-interviews-strategies-road-map-2015-2025/376>, **2015**.
- [9] “Supercapacitor Technologies and Markets 2016-2026,” can be found under <http://www.idtechex.com/research/reports/supercapacitor-technologies-and-markets-2016-2026-000486.asp>, **2016**.
- [10] A. Burke, *International Journal of Energy Research* **2010**, *34*, 133.
- [11] M. D. Stoller, R. S. Ruoff, *Energy Environ. Sci.* **2010**, *3*, 1294.
- [12] A. Burke, M. Miller, *Electrochimica Acta* **2010**, *55*, 7538.
- [13] M. Conte, *Fuel Cells* **2010**, *10*, 806.
- [14] Y. Gogotsi, P. Simon, *Science* **2011**, *334*, 917.
- [15] T. S. Mathis, N. Kurra, X. Wang, D. Pinto, P. Simon, Y. Gogotsi, *Advanced Energy Materials* **2019**, *9*, 1902007.
- [16] A. Noori, M. F. El-Kady, M. S. Rahmanifar, R. B. Kaner, M. F. Mousavi, *Chem. Soc. Rev.* **2019**, *48*, 1272.

- [17] J. Xie, P. Yang, Y. Wang, T. Qi, Y. Lei, C. M. Li, *Journal of Power Sources* **2018**, *401*, 213.
- [18] A. Laheäär, P. Przygocki, Q. Abbas, F. Béguin, *Electrochemistry Communications* **2015**, *60*, 21.
- [19] C. Arbizzani, Y. Yu, J. Li, J. Xiao, Y. Xia, Y. Yang, C. Santato, R. Raccichini, S. Passerini, *Journal of Power Sources* **2020**, *450*, 227636.
- [20] S. Razoumov, A. Klementov, S. Litvinenko, A. Beliakov, *Asymmetric Electrochemical Capacitor and Method of Making*, **2001**, US6222723B1.
- [21] G. G. Amatucci, F. Badway, A. D. Pasquier, T. Zheng, *J. Electrochem. Soc.* **2001**, *148*, A930.
- [22] J. P. Zheng, *J. Electrochem. Soc.* **2003**, *150*, A484.
- [23] J. Ding, W. Hu, E. Paek, D. Mitlin, *Chem. Rev.* **2018**, *118*, 6457.
- [24] H. Wang, C. Zhu, D. Chao, Q. Yan, H. J. Fan, *Advanced Materials* **2017**, *29*, 1702093.
- [25] G. Li, Z. Yang, Z. Yin, H. Guo, Z. Wang, G. Yan, Y. Liu, L. Li, J. Wang, *J. Mater. Chem. A* **2019**, *7*, 15541.
- [26] A. Jagadale, X. Zhou, R. Xiong, D. P. Dubal, J. Xu, S. Yang, *Energy Storage Materials* **2019**, *19*, 314.
- [27] W. Zuo, R. Li, C. Zhou, Y. Li, J. Xia, J. Liu, *Advanced Science* **2017**, *4*, 1600539.
- [28] N. Omar, J. Ronsmans, Y. Firozu, M. A. Monem, A. Samba, H. Gualous, O. Hegazy, J. Smekens, Th. Coosemans, P. Van den Bossche, J. Van Mierlo, in *2013 World Electric Vehicle Symposium and Exhibition (EVS27)*, **2013**, 1–11.
- [29] J. R. Miller, *Journal of Power Sources* **2016**, *326*, 726.
- [30] T. Tsuda, N. Ando, N. Mitsuhashi, T. Tanabe, K. Itagaki, N. Soma, S. Nakamura, N. Hayashi, F. Matsumoto, *ECS Trans.* **2017**, *77*, 1897.
- [31] J. Come, V. Augustyn, J. W. Kim, P. Rozier, P.-L. Taberna, P. Gogotsi, J. W. Long, B. Dunn, P. Simon, *J. Electrochem. Soc.* **2014**, *161*, A718.

- [32] K. Pfeifer, S. Arnold, J. Becherer, C. Das, J. Maibach, H. Ehrenberg, S. Dsoke, *ChemSusChem* **2019**, *12*, 3312.
- [33] T. Aida, K. Yamada, M. Morita, *Electrochem. Solid-State Lett.* **2006**, *9*, A534.
- [34] L. Jin, C. Shen, A. Shellikeri, Q. Wu, J. Zheng, P. Andrei, J.-G. Zhang, J. P. Zheng, *Energy Environ. Sci.* **2020**, *13*, 2341-2362.
- [35] M. Arnaiz, J. Ajuria, *Batteries & Supercaps* **2021**.
- [36] J. Zhang, Z. Shi, C. Wang, *Electrochimica Acta* **2014**, *125*, 22.
- [37] T. Watanabe, T. Tsuda, N. Ando, S. Nakamura, N. Hayashi, N. Soma, T. Gunji, T. Ohsaka, F. Matsumoto, *Electrochimica Acta* **2019**, *324*, 134848.
- [38] P. Jeżowski, O. Crosnier, E. Deunf, P. Poizot, F. Béguin, T. Brousse, *Nat. Mater.* **2018**, *17*, 167.
- [39] M. Arnaiz, D. Shanmukaraj, D. Carriazo, D. Bhattacharjya, A. Villaverde, M. Armand, J. Ajuria, *Energy Environ. Sci.* **2020**, *13*, 2441-2449.
- [40] N. El Ghossein, A. Sari, P. Venet, *IEEE Transactions on Power Electronics* **2017**, *1*.
- [41] D. G. Moye, P. L. Moss, X. J. Chen, W. J. Cao, S. Y. Foo, *Journal of Power Sources* **2019**, *435*, 226694.
- [42] A. Slesinski, K. Fic, E. Frackowiak, *Advances in Inorganic Chemistry* **2018**, 247–286.
- [43] J. Ajuria, E. Redondo, M. Arnaiz, R. Mysyk, T. Rojo, E. Goikolea, *Journal of Power Sources* **2017**, *359*, 17.
- [44] M. Arnaiz, J. L. Gómez-Cámer, F. Mijangos, T. Rojo, E. Goikolea, J. Ajuria, *Batteries & Supercaps* **2019**, *2*, 153.
- [45] J. L. Gómez-Cámer, M. Arnaiz, T. Rojo, J. Ajuria, *Journal of Power Sources* **2019**, *434*, 226695.
- [46] M. Lu, F. Beguin, E. Frackowiak, *John Wiley & Sons* **2013**.
- [47] J. Zhao, Y. Gao, A. F. Burke, *Journal of Power Sources* **2017**, *363*, 327.



Dr. Leire Caizán is currently a Post-doctoral Researcher at CICenergiGUNE-energy cooperative research center. She obtained her Ph.D. degree in 2019 at the University of Wageningen. Her research interest is to characterize electrochemical systems such as capacitors, batteries and fuel cells towards their optimization and application for energy storage and conversion purposes.



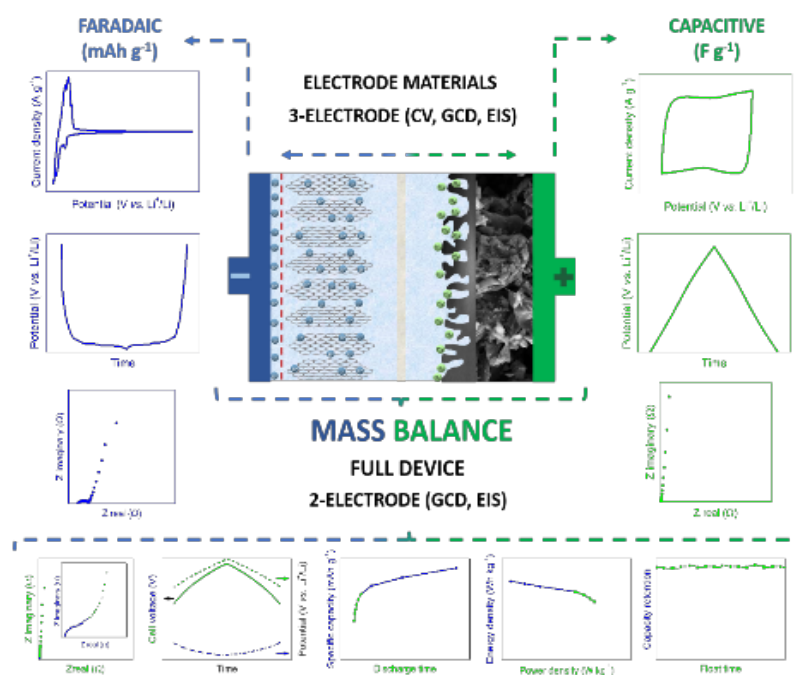
Dr. María Arnaiz is currently a Post-doctoral Researcher at CICenergiGUNE-energy cooperative research center. She obtained her Ph.D. degree in 2019 at the University of the Basque Country. Her research interest is focused on the development and up-scaling of metal-ion capacitors, with special focus set on electrode processing and full cell assembly, characterization and optimization.



Dr. Jon Ajuria is currently Associate Researcher at CICenergiGUNE-energy cooperative research center. He obtained his Ph.D. in 2012 at the University of the Basque Country. His research interests include energy storage materials and devices, but especially metal-ion capacitors, from basic concepts to the development of prototypes.

Leire Caizán-Juanarena<sup>1</sup>, María Arnaiz<sup>1</sup>, Emanuele Gucciardi<sup>1</sup>, Laura Oca<sup>1</sup>, Emilie Bekaert<sup>1</sup>,  
 Iñigo Gandiaga<sup>2</sup>, Jon Ajuria<sup>1,\*</sup>

## Unraveling the Technology behind the Frontrunner LIC ULTIMO® to Serve as a Guideline for Optimum Lithium-ion Capacitor Design, Assembly and Characterization



A bright future waits for lithium-ion capacitors. Academic research is growing exponentially and a widespread market entry is foreseen during the following years. However, history is repeating itself and errors made in the past by its sister EDLC technology seems to be repeating nowadays. Thus, the aim of the following report is to refresh research focus and to serve as a guideline for the appropriate design and reporting of LICs.

## Supporting Information

### Unraveling the Technology behind the Frontrunner LIC ULTIMO<sup>®</sup> to Serve as a Guideline for Optimum Lithium-ion Capacitor Design, Assembly and Characterization

Leire Caizán-Juanarena<sup>1</sup>, María Arnaiz<sup>1</sup>, Emanuele Gucciardi<sup>1</sup>, Laura Oca<sup>1</sup>, Emilie Bekaert<sup>1</sup>, Iñigo Gandiaga<sup>2</sup>, Jon Ajuria<sup>1,\*</sup>

#### Electrical characterization of LIC ULTIMO<sup>®</sup>

Prior to the characterization of the materials of which LIC ULTIMO<sup>®</sup> is composed a detailed electrical characterization of a prismatic 2300 F LIC ULTIMO<sup>®</sup> was conducted (**Table S1**). The characterization was done in laboratory environment, using a Peltier effect based Prebatem Selecta thermal chamber and Digatron MCT 100-6-10 battery tester.

**Table S1.** Specifications of prismatic 2300 F and 3300 F LIC ULTIMO<sup>®</sup>

	Capacitance	2300 F	3300 F	Conditions
				Ambient temperature: 25 °C Discharge current at: 10 A
Initial characteristics	DC-IR	0.7 mΩ	1.0 mΩ	
	Gravimetric energy density	8 Wh kg <sup>-1</sup>	14 Wh kg <sup>-1</sup>	
	Volumetric energy density	14 Wh L <sup>-1</sup>	20 Wh L <sup>-1</sup>	
	Gravimetric power density	8 kW kg <sup>-1</sup>	8 kW kg <sup>-1</sup>	With maximum discharge current
	Volumetric power density	14 kW L <sup>-1</sup>	12 kW L <sup>-1</sup>	
	Maximum discharge current	1200 A	1100 A	Discharge current can be continued for 1s
	Temperature characteristics	Lowest temperature in the temperature range	70 %	75 %
Highest temperature in the temperature range		100 %	100 %	
Self-discharge	Voltage drop after 10,000h stored	<5 %	<5 %	Ambient temperature: 25 °C Initial voltage: 3 V
Cycle durability	Cycle counts required to 80% capacitance retention	>1,000,000 cycles	>500,000 cycles	Ambient temperature: 25 °C Cycling current: 200 A Conditions: constant current, continuous
Operating temperature range		-30 °C ~ 70 °C	-30 °C ~ 70 °C	
Dimensions in mm		150.2 x 93.2 x 15.8	150.2 x 93.2 x 15.8	Without terminal tabs and fixing studs
Weight		0.36 kg	0.32 kg	

The electrical performance study was carried out by charging and discharging the cells at different constant currents rates (10 A, 100 A, 200 A, 400 A) and at different temperatures (-30 °C, -10 °C, 15 °C, 25 °C, 35 °C and 45 °C). **Figure S1** shows the results of the discharging rate capability tests that were carried out at 25 °C. Applied charging protocol was based on a constant current of 10 A up to 3.8 V followed by a constant voltage step down to 0.5 A. All tests were conducted at high current rates (*i.e.* 10 A, 100 A, 200 A, and 400 A) if compared to those use in batteries, where the lowest charge and discharge rate was of 10 C. Electrochemical tests were followed in the fast discharging and charging area, *i.e.* complete discharge of the LIC in 7 s at 400 A (**Figure S1a**). At 10 A, the cell discharges 100 % of its nominal storing capacity (1.025 Ah), while at higher current rates the discharged capacity is reduced to 93.7 %, 87.8 % and 76.7 % at 100 A, 200 A and 400 A respectively (**Figure S1b**). At higher current rates, the shape of the voltage hardly changes, except for the initial drop in voltage affected by the Equivalent Series Resistance (ESR), and the obtained voltage curves are parallel between them. This indicates that the cell hardly loses energy by dissipation and that the difference between discharge currents is only relative to the ESR. Similar results were obtained at different temperatures and even changing the charging current.

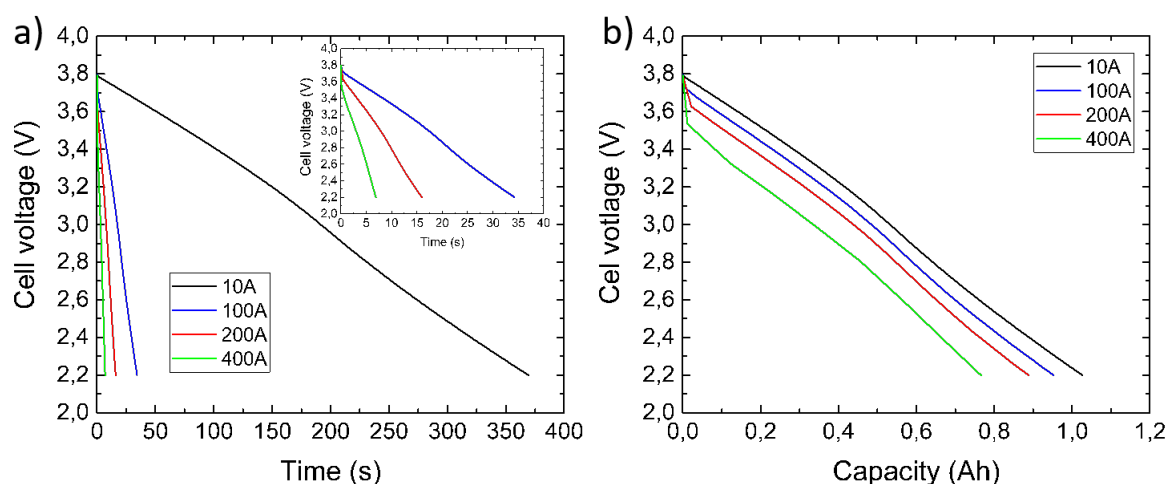


**Figure S1.** Rate capability test carried out to prismatic 2300 F LIC ULTIMO<sup>®</sup> under different applied currents at room temperature: a) discharge profiles, inset: zoom fast discharge region and b) capacity values.

Ageing analysis is one of the key issues for this technology, as long useful lifetime guarantee is required for target applications based EES improvement. Cycling ageing analysis at high current rate (*i.e.* 50 A, around 1 min charge and 1 min discharge) and high ambient temperature (*i.e.* 45 °C) was done with the objective of verifying the cyclability of the LIC ULTIMO<sup>®</sup>

technology. As depicted in **Figure S2**, the 2300 F LIC ULTIMO<sup>®</sup> only loses 5 % of its initial capacity after almost 1000000 cycles (more than 3 years of testing) at high current and temperature with a depth of discharge (DOD) of 100 %. On one hand, compared to a Li-ion battery, there is no doubt that this storage system is far above the state of the art in lifetime. On the other hand, when comparing it with UCs, it can be concluded that this LIC has an improved life behaviour, since it does not suffer such a big loss of its initial capacity, while in UCs initial capacity losses of more than 10 % are reported. Regarding the internal resistance, it is worth mentioning that the cell did not suffer any change after 1000000 full cycles. Taking into account these results it can be concluded that the 2300 F LIC ULTIMO<sup>®</sup> meets the original targets set for LICs.

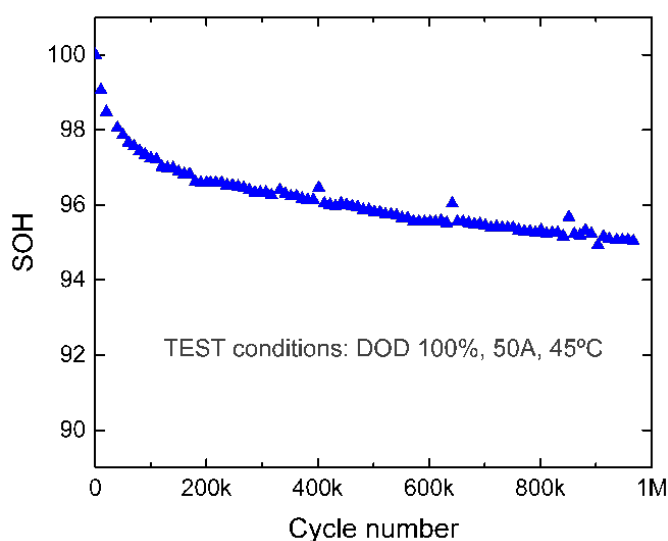


**Figure S2.** Cyclability test carried out to 2300 F LIC ULTIMO<sup>®</sup> at 50 A and 45 °C

### Ante-mortem characterization of LIC ULTIMO<sup>®</sup>

LIC ULTIMO<sup>®</sup> was opened inside a Jacomex glovebox at a cell voltage of 2.2 V, after ensuring its complete discharge by a constant current (1 C) followed (twice) by a constant voltage (2.2 V) hold of 30 minutes and a constant current discharge at a lower rate (0.2 C). The cell was opened within the next 3 h following the post-mortem procedure of LIBs in literature. Firstly, the electrolyte was extracted from the security valve located on top of the metallic case, in order to avoid the short-circuit of the device. Secondly, a horizontal cut was made across the metallic case with a semicircular diamond saw blade, which allowed the extraction of the inner jelly-roll. Thirdly, both electrode terminals, including the two metallic pins that served to join all positive and negative electrodes, were removed. Last, all cell components were unrolled,



separated and stored for their further drying and characterization (see **Figure S3** for the opening procedure).

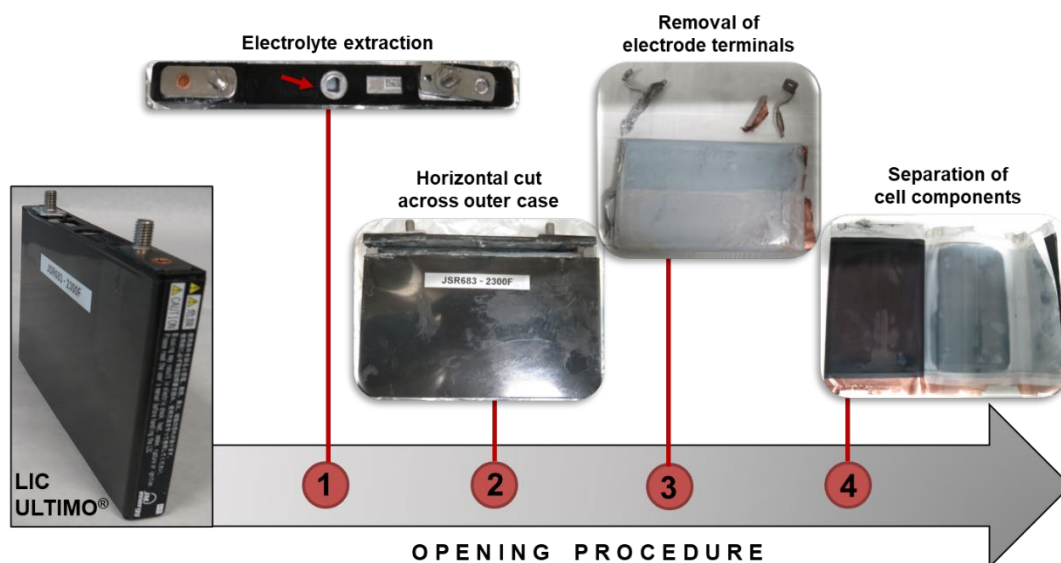


**Figure S3.** Opening procedure of 2300 F LIC ULTIMO®

The outer metallic case weighed 0.36 kg and had the following dimensions: 150.2 x 93.2 x 15.8 mm, in good agreement with reported specifications (see **Table S1**). The electrodes were packed in a prismatic configuration with the following components in the following order: i) separator, ii) pre-lithiation plate, iii) negative electrode (graphite as active material coated on top of a copper current collector), iv) positive electrode (activated carbon as active material coated on top of an aluminum current collector), and v) an inner plastic that held all the rolled structure. The negative and positive electrodes were thereafter measured for their length, height and thickness, and they were similarly weighted after a washing process with dimethyl carbonate (DMC) to remove the electrolyte salt. Several electrode pieces (of a known area of 1.13 cm<sup>2</sup>) were weighted to calculate the standard deviation of the measurements. The average weight of these electrode pieces was used to extrapolate the weight of the total electrode area. Same procedure was followed for both current collectors after removing the 2-sided coated electrode material with N-Methyl-2-pyrrolidone (NMP). Note that the copper current collector covers 30% less area due to the holes (see **Figure S4**), while on the contrary the graphite increases its total volume as it is filling up the space within these holes. Finally, the geometrical dimensions and weight of the pre-lithiation plate and separator were also determined. It can be said that both electrodes present high active material loadings well beyond 90 %. In addition, they present extremely small particle size distribution and extremely high purity and small

particle size distribution. X-ray diffraction (XRD) of the powdered electrodes allowed us to confirm the high crystallinity and purity of graphite as well as the amorphous nature of the activated carbon.

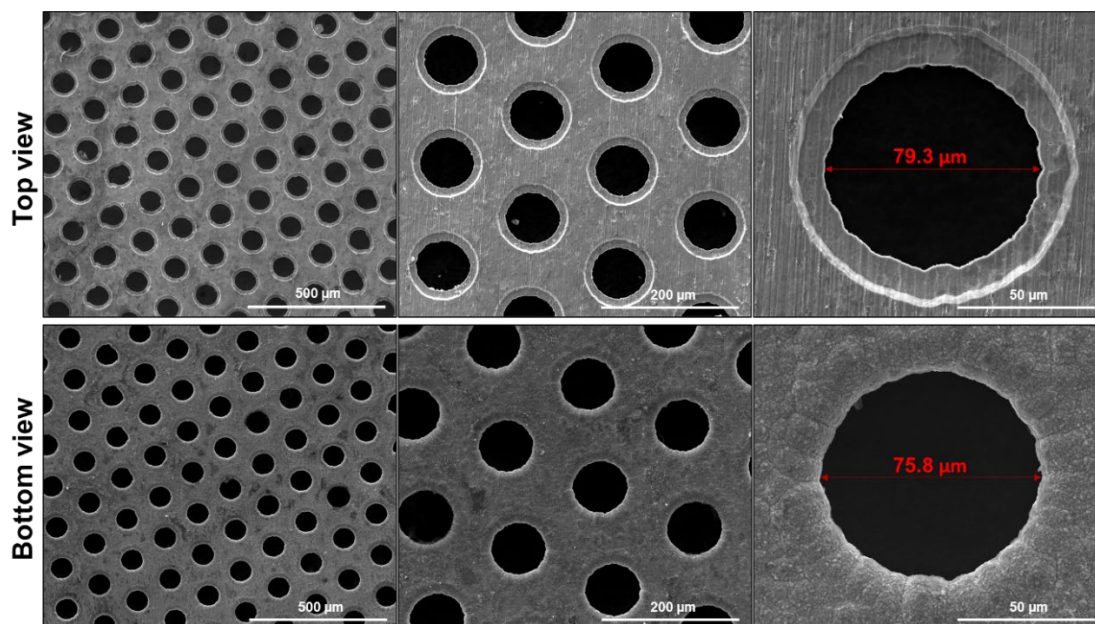


**Figure S4.** Microstructural characterization of the pre-lithiation copper plate from both top and bottom views.

Electrodes were further characterized for their porous structure by means of helium pycnometry, nitrogen/carbon dioxide gas adsorption/desorption and mercury porosimetry. These techniques are meant to provide complementary information about the micro-, meso- and macro-porosity of materials and thereby, their specific surface area (SSA), which determines the electrolyte-electrode interface participating in both capacitive (AC) and faradaic (graphite) energy storage processes. The SSA for the positive electrode (AC + conducting agent + binder) was in the range typical for commercial ACs, with a nanometric average pore size ( $\text{N}_2$  adsorption), while the SSA was low for the negative electrode (graphite + conducting agent + binder), with a sub nanometric average pore size ( $\text{CO}_2$  adsorption). These values were expected since the activated carbon is known to have a high SSA for the formation of electrical double-layer (EDL), while the graphite does not need micro-porosity in the graphene layers for  $\text{Li}^+$  insertion. Apart from the intrinsic porosity of carbon materials, macro-porosity of the coating once casted on the current collector is also important as it can determine the final performance of the LIC. For that reason, Hg porosimetry was used to investigate the macro-porosity. Both electrodes showed a

bulk density value similar to the apparent density, meaning little added macroporosity was found in the laminated electrodes.

Apart from electrodes, other cell constituents were also analyzed, such as the separator or the electrolyte. Regarding the separator, its composition was determined by using infrared spectroscopy technique and was found to be polymeric (see **Figure S5**).

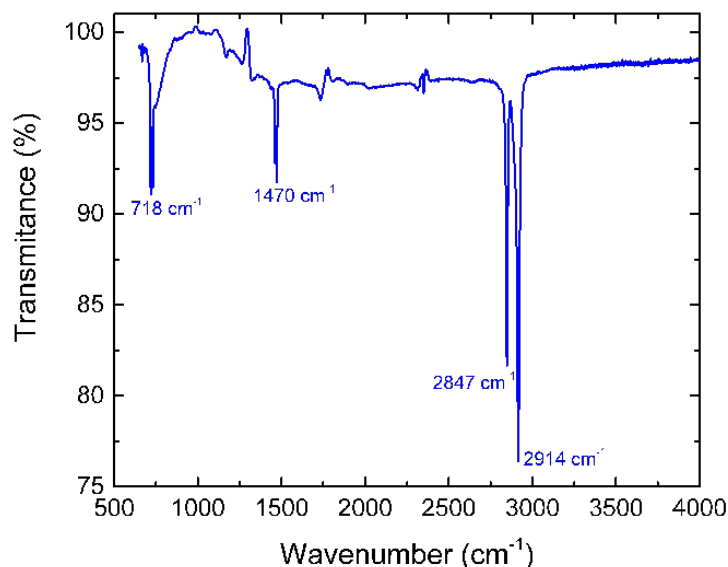


**Figure S5.** Fourier-transform infrared (FTIR) transmission spectrum of the separator.

Regarding the electrolyte, this was determined by gas chromatography and mass spectroscopy (GC-MS) and the following components were identified: dimethyl carbonate (DMC), ethyl carbonate (EC) and ethyl methyl carbonate (EMC) (**Figure S6a**). Liquid NMR was also followed in order to identify the salt used, which was  $\text{LiPF}_6$  (**Figure S6b**). Finally, ionic conductivity of the electrolyte at room temperature was determined as  $9.1 \pm 0.2 \text{ mS cm}^{-1}$  with electrochemical impedance spectroscopy (EIS); two parallel electrode plates ( $L/A = 1.6 \text{ cm}$ ) were submerged in the electrolyte, where a constant potential (0.00 V) EIS was performed (in triplicate) in the frequency range of 1-100 Hz (Amplitude = 10 mV; Number of decades = 6). A linear fit was done to the Nyquist plot, where the X intercept of the semicircle gave the value of resistance ( $R_\Omega$ ) needed to calculate ionic conductivity ( $\sigma = 1.6/R_\Omega$ ).

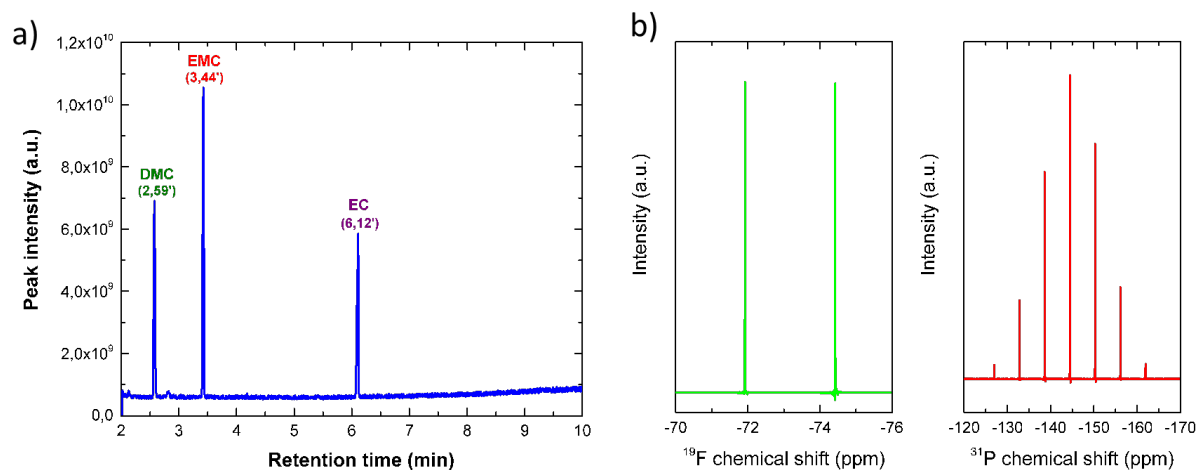


**Figure S6.** Electrolyte composition determined by a) GC-MS and b) liquid NMR to identify main solvents (DMC, EMC and EC) and the salt ( $\text{LiPF}_6$ ).

### Guideline for proper reporting of electrode materials and LICs

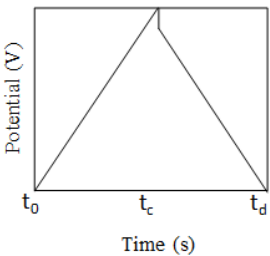
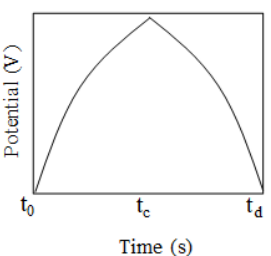
Formulas for electrode materials evaluation (Table S2) and LIC evaluation (Table S3) are presented, where  $Q$  is the stored charge (mAh),  $m$  the mass of the active material (mg),  $\Delta t$  is the difference between charge ( $t_c$ ) and discharge time ( $t_d$ ) (s),  $\Delta V$  is the potential window (V),  $I$  is the discharge current (mA).

**Table S2.** Formulas used to calculate electrochemical performance of electrode materials.

\*N/A: not applicable

Electrode materials			
	Capacitive	Pseudocapacitive	Faradaic
Capacitance	$C (F g^{-1}) = \frac{Q}{m \cdot V} = \frac{I \cdot \Delta t}{m \cdot \Delta V}$	N/A	
Capacity	$C (mA h g^{-1}) = \frac{3,6 \cdot Q}{m} = \frac{3,6 \int_0^{t_d} I(t) \cdot dt}{m}$		
Coulombic efficiency	$CE (\%) = \frac{Q_d}{Q_c} \cdot 100 = \frac{\int_0^{t_d} I(t) \cdot dt}{\int_0^{t_c} I(t) \cdot dt} \cdot 100$		
Equivalent Series resistance	$ESR (\Omega) = \frac{\Delta V_{ESR}}{ I_c  +  I_d } \quad // \quad ESR (\Omega) = \frac{\Delta V_{ESR}}{ I_d }$		

**Table S3.** Formulas used to calculate electrochemical performance of electrochemical devices (LICs). \*N/A: not applicable

<b>Lithium Ion Capacitors</b>		
	Symmetric	Assymmetric
	 <p>Potential (V)</p> <p>Time (s)</p>	 <p>Potential (V)</p> <p>Time (s)</p>
Capacitance	$C (F g^{-1}) = \frac{Q}{m \cdot V} = \frac{I \cdot \Delta t}{m \cdot \Delta V}$	N/A
Capacity	$C (mA h g^{-1}) = \frac{3,6 \cdot Q}{m} = \frac{3,6 \int_0^{t_d} I(t) \cdot dt}{m}$	
Coulombic efficiency	$CE (\%) = \frac{Q_d}{Q_c} \cdot 100 = \frac{\int_0^{t_d} I(t) \cdot dt}{\int_0^{t_c} I(t) \cdot dt} \cdot 100$	
Equivalent Series resistance	$ESR (\Omega) = \frac{\Delta V_{ESR}}{ I_c  +  I_d } \quad // \quad ESR (\Omega) = \frac{\Delta V_{ESR}}{ I_d }$	

Where  $Q$  is the stored charge (mAh),  $m$  the mass of the active material (mg),  $\Delta t$  is the difference between charge ( $t_c$ ) and discharge time ( $t_d$ ) (s),  $\Delta V$  is the potential window (V),  $I$  is the discharge current (mA).